biosensors

MDPI

Communication

Label-Free Fluorescent Turn-On Glyphosate Sensing Based on DNA-Templated Silver Nanoclusters

Yuliang Cheng [1,2,†], Guowen Li [1,2,†], Xiufang Huang [1,2], Zhijuan Qian [3] and Chifang Peng [1,2,4,*]

[1] State Key Laboratory of Food Science and Technology, Jiangnan University, Lihu Road 1800, Wuxi 214122, China
[2] School of Food Science and Technology, Jiangnan University, Lihu Road 1800, Wuxi 214122, China
[3] Nanjing Customs District Light Industry 375 Productsand Children's Products Inspection Center, Yangzhou 225009, China
[4] International Joint Laboratory on Food Safety, Jiangnan University, Lihu Road 1800, Wuxi 214122, China
* Correspondence: pcf@jiangnan.edu.cn; Tel.: +86-510-85329081
† These authors contributed equally to this work.

Abstract: In this work, a label-free fluorescent detection method for glyphosate, based on DNA-templated silver nanoclusters (DNA-Ag NCs) and a Cu^{2+}-ion-modulated strategy, was developed. In the presence of Cu^{2+}, the fluorescence of the DNA-Ag NCs was quenched. Glyphosate can restore the fluorescence of DNA-Ag NCs. By analyzing the storage stability of the obtained DNA-Ag NCs using different DNA templates, specific DNA-Ag NCs were selected for the construction of the glyphosate sensor. The ultrasensitive detection of glyphosate was achieved by optimizing the buffer pH and Cu^{2+} concentration. The sensing of glyphosate demonstrated a linear response in the range of 1.0–50 ng/mL. The limit of detection (LOD) was 0.2 ng/mL. The proposed method was successfully applied in the detection of glyphosate in a real sample, indicating its high application potential for glyphosate detection.

Keywords: label free; fluorescence; turn on; DNA; Cu^{2+}; silver nanoclusters

Citation: Cheng, Y.; Li, G.; Huang, X.; Qian, Z.; Peng, C. Label-Free Fluorescent Turn-On Glyphosate Sensing Based on DNA-Templated Silver Nanoclusters. *Biosensors* **2022**, *12*, 832. https://doi.org/10.3390/bios12100832

Received: 26 August 2022
Accepted: 3 October 2022
Published: 6 October 2022

1. Introduction

Glyphosate, a broad-spectrum organophosphorus herbicide, is the largest pesticide by sales in the global crop protection market. It is widely used around the world and mainly used for weed removal before crop planting. There is increasing evidence that glyphosate is potentially toxic to non-target organisms [1]. In 2017, the International Agency for Research on Cancer (IARC) classified glyphosate as a possible human carcinogen [2]. Glyphosate applied in agricultural environments can enter the water environment through various ways [3]. In recent years, glyphosate has been found in surface water worldwide. Therefore, the determination of glyphosate in water is very important.

Some conventional analytical methods such as high-performance liquid chromatography [4] and mass spectrometry [5] are commonly used for the determination of pesticide residues in foods. Although these methods provide accurate and sensitive results, we have to tolerate their disadvantages, including their complicated operation and requirement of professional personnel. Therefore, there is a growing need to establish simple, rapid, sensitive, and low-cost sensing methods for glyphosate, which benefit on-site detection in resource-limited scenarios.

DNA template nanosensors exhibit excellent optical properties, including high-fluorescence quantum yield and stability, biocompatibility, ease of synthesis, and low toxicity. By changing the DNA sequence and structure, the DNA template nanosensors could be used for the detection of different targets [6]. The various DNA template silver nanoclusters (DNA-Ag NCs) with fluorescence emission from the UV to near-infrared regions could also be synthesized based on changing the DNA sequence and environmental

factors [7]. DNA-Ag NCs have been applied in the detection of a variety of targets, such as heavy metal ions [8], proteins [9], viruses, microRNAs [10], and thiols [11]. However, few studies have been involved in the application of DNA-Ag NCs in the enzyme-free fluorescent detection of pesticides.

Herein, we developed a fluorescent detection glyphosate based on DNA-Ag NCs. In the presence of Cu^{2+}, which can bind to the DNA template through the electrostatic interaction with the phosphate group and basic bases, the fluorescence of the DNA-Ag NCs was quenched. However, glyphosate can trap Cu^{2+} and greatly restore the fluorescence of DNA-Ag NCs. Thus, the DNA-Ag NC-based "turn-on" fluorescent sensing of glyphosate was realized (Figure 1). Moreover, we found specific DNA-templated Ag NCs that demonstrated excellent storage stability and were suitable for the above glyphosate sensing strategy.

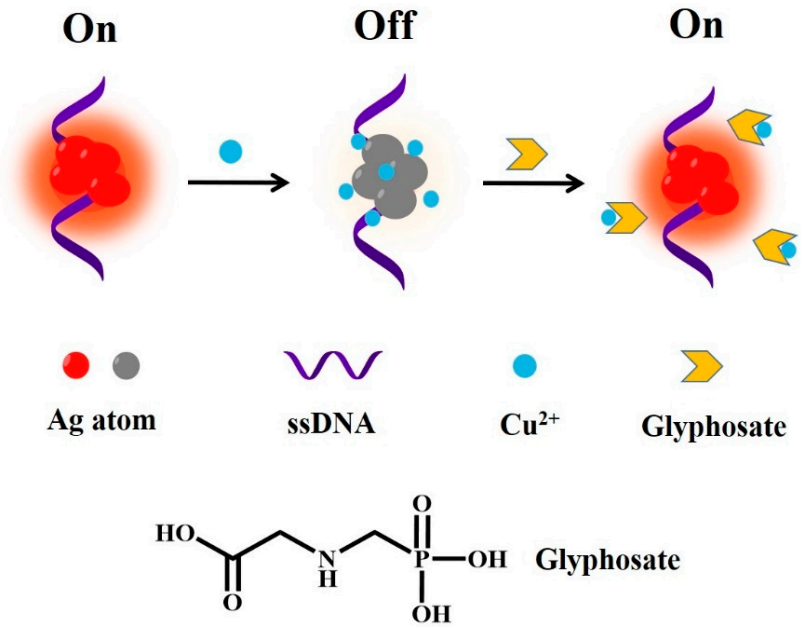

Figure 1. Schematic illustration of the detection of glyphosate based on DNA-Ag NCs.

2. Materials and Apparatus

2.1. Chemicals and Reagents

All chemicals were used directly without any further purification, and all chemical reagents in this experiment were of analytical grade. Sodium borohydride ($NaBH_4$), silver nitrate ($AgNO_3$), zinc nitrate hexahydrate ($Zn(NO_3)_2{\cdot}6H_2O$), iron nitrate hexahydrate ($Fe(NO_3)_3{\cdot}9H_2O$), lead nitrate ($Pb(NO_3)_2$), nickel sulfate hexahydrate ($NiSO_4{\cdot}6H_2O$), manganese chloride tetrahydrate ($MnCl_2{\cdot}4H_2O$), aluminum nitrate hexahydrate ($Al(NO_3)_3{\cdot}9H_2O$), mercury nitrate ($Hg(NO_3)_2$), cobalt nitrate ($Co(NO_3)_2$), ethylene diamine tetra-acetic acid (EDTA), 5-morinopropanulfonic acid (MOPs), and sodium hydroxide (NaOH) were purchased from Shanghai Aladdin Biochemical Technology Co., Ltd. (Shanghai, China). All experimental water resistance values were higher than 18 MΩ/cm. All pesticides were purchased from Shanghai Pesticide Research Institute (Shanghai, China). The template DNA was synthesized by Sangon Bioengineering (Shanghai, China) Co. Sangon Bioengineering Co., Ltd. (Shanghai, China)

2.2. Apparatus

The transmission electron microscope (TEM) images of DNA-Ag NCs were obtained using a JEOL-2100 transmission electron microscope (Japan Electron Optics Laboratory Co., Ltd., Tokyo, Japan). The fluorescence spectra were measured using a F97Pro fluorescence spectrophotometer (Shanghai Ling Guang Technology Co., Ltd., Shanghai, China). The

circular dichroism (CD) spectra were recorded by Chirascan V100 (Applied Photophysics, Surrey, UK). The weight measurements were carried out via analytical balance (MS105DU, Mettler Toledo Instruments Shanghai Co., Ltd., Shanghai, China).

3. Experimental Method

3.1. Preparation of DNA-Ag NCs

The DNA-Ag NCs were synthesized through the one-step method. Briefly, 16 μL of DNA (250 μmol /L) was mixed with 166 μL of phosphate buffer (PB, 20 mM, pH = 7.0) and 6 μL of $AgNO_3$ (4 mM) under vigorous stirring, and then the mixture was incubated at 4 °C for 20 min. Then, 12 μL of $NaBH_4$ (2 mmol/L) prepared with ice water was added to the mixture under vigorous stirring and then incubated at room temperature for 3 h in the dark. Finally, the obtained DNA-Ag NCs were stored at 4 °C for future use.

3.2. Protocol of the Glyphosate Detection

Different concentrations of glyphosate (5 μL) were mixed with 20 μL of Cu^{2+} (300 nM) in 10 mM MOPS buffer (pH 7.5) and incubated for 2 min. Subsequently, 60 μL of DNA-Ag NC solution and 15 μL of MOPS buffer (pH 7.5) were added. The final volume of the mixture was 100 μL. After incubation for 25 min at the room temperature, the fluorescence intensity of the mixture was recorded using a fluorescence spectrophotometer.

3.3. Glyphosate Detection in Real Samples

Tap water and spring water were collected from the lab and supermarket as real samples. Different concentrations of glyphosate (5 ng/mL, 20 ng/mL, and 40 ng/mL) were added to the samples and filtered with a 0.22 μm microporous membrane. The fluorescence emission spectra were recorded and the recovery rates were calculated.

4. Results and Discussion

4.1. Sensing Strategies for Glyphosate Detection

The interactions of metal cations with nucleic acid have been used in the design of DNA-based nanosensors [12]. It was reported that Cu^{2+} was mainly attached to the phosphate group of nucleic acids and also can bind to the basic groups of nucleic acid [13]. Cu^{2+} mainly binds to the N7 and O6 positions of guanine and the O2 position of cytosine [14]. Ag^{+} can specifically bind to the N3 site of cytosine [15]. Compared with adenine (A), guanine (G), and thymine (T) bases, Ag^{+} towards the cytosine (C) base showed much a higher binding affinity. The binding constants of C-Ag^{+}-C base pairs can be compared with T-Hg^{2+}-T base pairs [16].

Based on the binding of Cu^{2+} to nucleic acid, we designed DNA-Ag NCs as a fluorescent probe to achieve rapid glyphosate detection through Cu^{2+}-mediated fluorescence modulation.

Cu^{2+} can bind to phosphate and basic groups in DNA, quenching the fluorescence of nanoclusters. In the presence of glyphosate, due to the strong binding affinity of the phosphonyl group (-PO_3H_2) and carboxyl group (-COOH) with Cu^{2+}, Cu^{2+} was trapped and the fluorescence of the DNA-Ag NCs was greatly restored.

4.2. Characterization of DNA-Ag NCs

The sequence and structure of the DNA template could greatly affect the fluorescence characteristic of DNA-Ag NCs [17]. For example, Dickson et al. obtained Ag NCs using five kinds of single-stranded DNA with similar sequences [18]. Yang et al. obtained silver nanoclusters with different emission wavelengths by adjusting the structural changes of the DNA template between a stem–loop structure and dimer [19]. The C-rich DNA sequence 5′-CCCTTAATCCCC-3′ was usually used as a template for the synthesis of DNA-Ag NCs. It was found that the G base could enhance the fluorescence of the C-rich DNA-Ag NCs. Therefore, we selected five typical C-rich DNA sequences reported in the literature. Two of them were inserted with multiple G bases (Table 1). They were evaluated for subsequent experiments.

Table 1. Sequences of five single-stranded DNA.

DNA	Sequence 5′-3′
DNA 1	*CCCTTAATCCCC*
DNA 2	ACCCGAACCTGGGCTACCA *CCCTTAATCCCC*
DNA 3	ATCCTCCCACC**GGG**CCTCCCACCATAAAAA *CCCTTAATCCCC*
DNA 4	GGCAGGTT**GGGG**TGACTAAAAA *CCCTTAATCCCC*
DNA 5	CTGACACCATATTATGAAGA *CCCTTAATCCCC*

As shown in Table 2, the maximum excitation wavelength and the maximum emission wavelength of the five DNA-Ag NCs showed great differences. The fluorescence intensity of the DNA2-Ag NCs, DNA3-Ag NCs, and DNA4-Ag NCs was higher than the other two Ag NCs (Figure 2), which was clearly observed under the 365 nm UV lamp (Figure 3).

Table 2. Excitation and emission wavelengths of different DNA-Ag NCs.

Name	λ_{ex}/nm	λ_{em}/nm
DNA1-Ag NCs	464	550
DNA2-Ag NCs	530	620
DNA3-Ag NCs	560	621
DNA4-Ag NCs	596	671
DNA5-Ag NCs	560	627

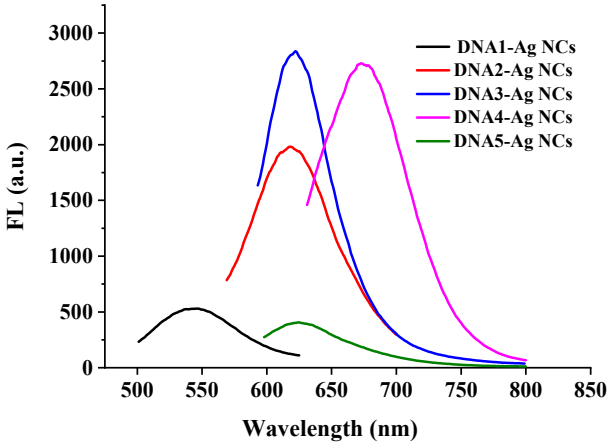

Figure 2. Fluorescence spectra of DNA-Ag NCs.

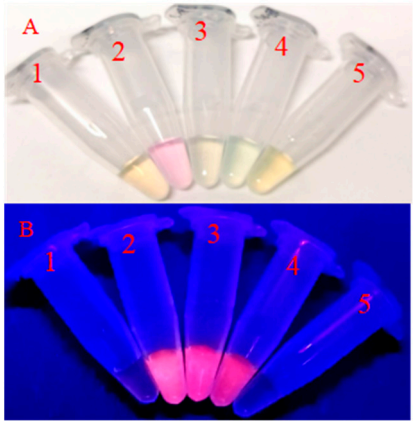

Figure 3. Digital images of DNA-Ag NCs illuminated with (**A**) white and (**B**) UV lights. 1–5 refer to the DNA1-Ag NCs to DNA5-Ag NCs.

The stability of Ag NCs is important for their practical applications. As shown in Figure 4, three kinds of DNA-Ag NCs were compared in terms of their stability. It was found that the fluorescence intensity of the DNA2-Ag NCs remained stable after being stored for 16 days. However, the fluorescence intensity of the DNA3-Ag NCs and DNA4-Ag NCs decreased by about 50% after 5 days. Therefore, we selected the DNA2-Ag NCs for the subsequent glyphosate detection.

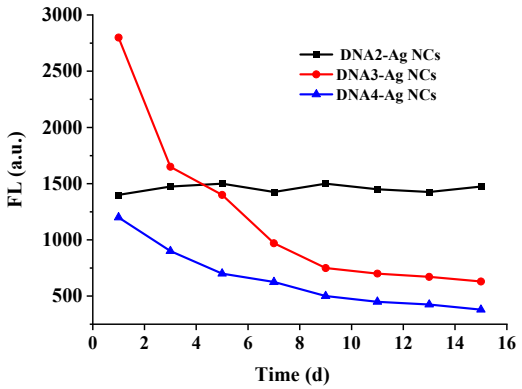

Figure 4. The stability of the prepared DNA-Ag NCs.

The morphology and particle size of the DNA2-Ag NCs were characterized via TEM and DLS. As shown in Figure 5, the synthesized DNA2-Ag NCs had no aggregation and the average particle size was about 2.2 nm.

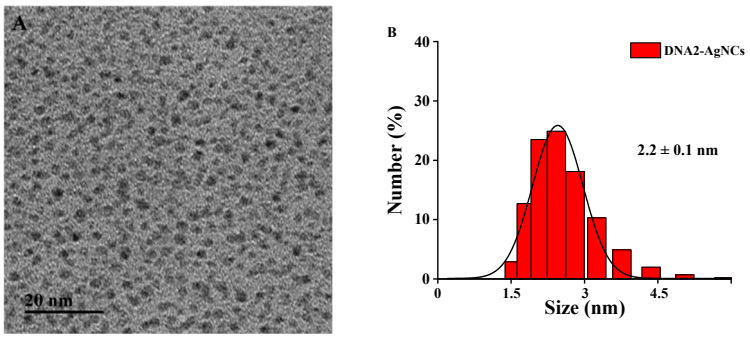

Figure 5. (**A**) TEM image of the DNA2-Ag NCs. (**B**) Particle size distribution histogram of the DNA2-Ag NCs.

As shown in Figure 6, the maximum excitation peak (λ_{ex}) of the DNA2-Ag NCs was at 530 nm and the maximum emission peak was at 620 nm.

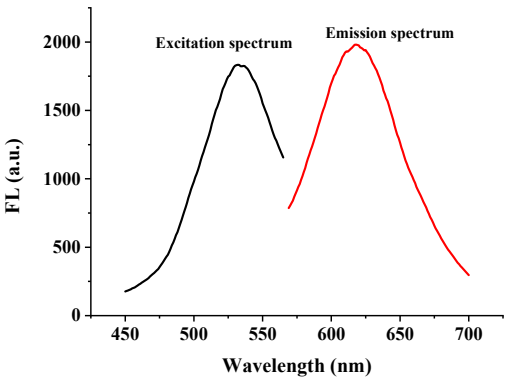

Figure 6. Fluorescence spectra of DNA2-Ag NCs.

4.3. Feasibility Verification of Glyphosate Detection

As shown in Figure 7, the DNA2-Ag NCs demonstrated a red fluorescence emission under 530 nm excitation. With the addition of the Cu^{2+} solution (60 nM), the fluorescence of the DNA2-Ag NCs was sharply quenched. In the presence of the glyphosate solution (500 ng/mL), the fluorescence of the DNA2-Ag NCs was significantly restored. However, the glyphosate alone had no significant effect on the fluorescence emission of the Ag NCs. Therefore, it is feasible to use Cu^{2+} to mediate the fluorescent detection of glyphosate based on the Ag NCs.

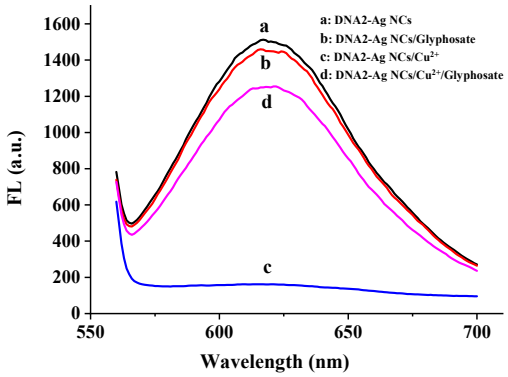

Figure 7. Fluorescence spectrum of DNA2-Ag NCs (a), DNA2-Ag NCs/glyphosate (b), DNA2-Ag NCs/Cu^{2+} (c), and DNA2-Ag NCs/Cu^{2+}/glyphosate (d).

4.4. Optimization of Sensing Conditions

The Cu^{2+} concentration towards the fluorescence quenching of the DNA2-Ag NCs was studied. As shown in Figure 8A,B, when the Cu^{2+} concentration was between 5 nM and 140 nM, the DNA2-Ag NCs quenching (F/F_0) gradually increased with the increased Cu^{2+} concentration (F_0 and F refer to the fluorescence intensity of the DNA2-Ag NCs in the absence and presence of Cu^{2+} ions, respectively). Meanwhile, the quenching efficiency ($(F_0 - F)/F_0$) reached 90% when the Cu^{2+} concentration was higher than 60 nM, which indicated that the fluorescence of the DNA2-Ag NCs was sensitive to the change in Cu^{2+} concentration. To further investigate the mechanism of the quenching effect, the Stern–Volmer equation was used [20]:

$$\frac{F_0}{F} = 1 + K_{SV}[Q] = 1 + k_q\tau_0 \quad (1)$$

Here, F_0 and F are the fluorescence intensity in the absence and presence of the quencher (Cu^{2+}), respectively; K_{sv} is the Stern–Volmer quenching constant, [Q] is the quencher concentration, and k_q is the quenching rate constant of the DNA-Ag NCs; τ_0 is the average excited-state lifetime of the DNA-Ag NCs, reported as 2.23 ns [18]. The linear regression of the F_0/F plot versus [Q] determines the K_{sv} value. As shown in Figure 8C, the Stern–Volmer plot is linear and the value of K_{sv} is 0.139. The k_q was calculated using the following equation:

$$k_q = \frac{K_{sv}}{\tau_0} \quad (2)$$

and the value of k_q was calculated to be 6.2×10^{16} M^{-1} s^{-1}, which was much higher than the maximum dynamic quenching constant (2.0×10^{10} M^{-1} s^{-1})[21]. Thus, the dynamic quenching was not predominated, since a complex was formed between the Cu^{2+} and DNA-Ag NCs. Therefore, static quenching was the predominant mechanism of the DNA-Ag NCs quenching in the presence of Cu^{2+}, which resulted in the complex formation.

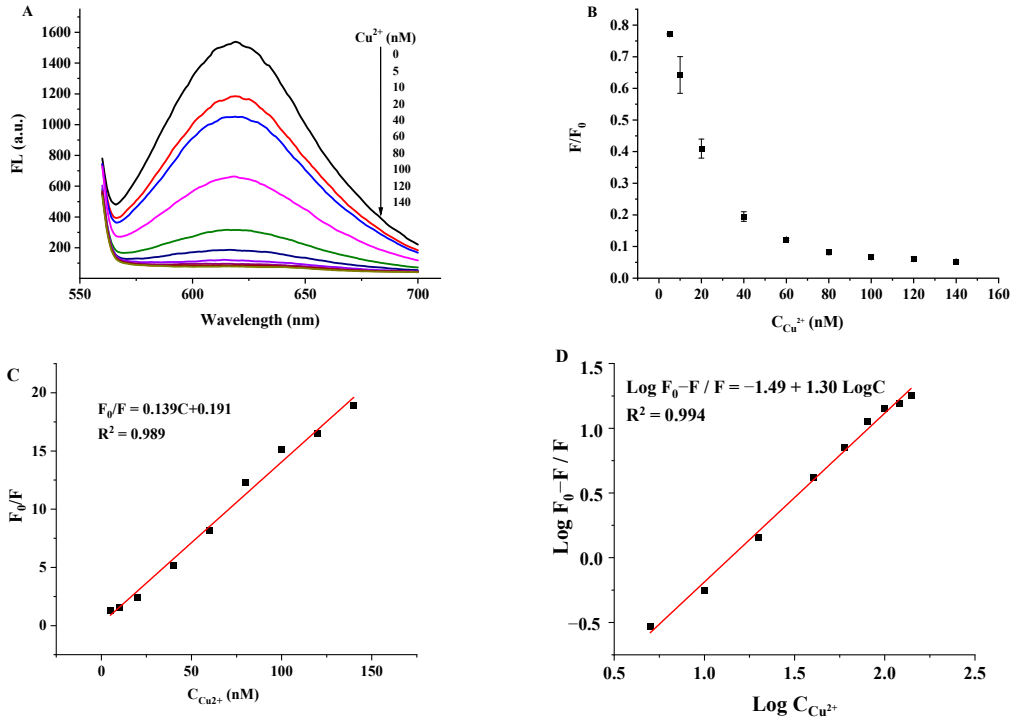

Figure 8. (**A**) The fluorescence quenching effect of DNA2-Ag NCs after adding Cu^{2+} (0 nM~140 nM). (**B**) The relationships between the F/F_0 and different concentrations of Cu^{2+}. (**C**) The Stern–Volmer plots of DNA2-AgNCs with Cu^{2+} F_0 and F are the fluorescence intensities of the DNA2-Ag NCs in the absence and presence of Cu^{2+}. (**D**) Computation of the binding constant (K) of each binding site and the number of binding sites of DNA-AgNCs (n).

In addition, the binding parameters of Cu^{2+} to DNA-Ag NCs were calculated using the following equation [22]:

$$\log[\frac{F_0 - F}{F}] = \log K + n \log[Q] \quad (3)$$

where n is the number of binding sites and K is the binding constant. As shown in Figure 8D, based on the plot of the double log graph of $[(F_0 - F)/F]$ versus log [Q], the values of n and K were obtained from the slope and Y-intercept, respectively. The result indicated that the binding constant between the DNA-Ag NCs and Cu^{2+} was 3.2×10^7 M^{-1}, which indicated that Cu^{2+} could bind to DNA-Ag NCs effectively. Madsen et al. analyzed the stability constants of several 1:1 metal complexes of glyphosate [23], and the stability constant ($LogK_{ML}$) for the Cu^{2+}-glyphosate complex was 11.92. Thus, the glyphosate binding to Cu^{2+} is much higher than for DNA-Ag NCs binding to Cu^{2+}. The stronger binding of the glyphosate to Cu^{2+} provided feasibility for the glyphosate sensing.

To evaluate the influence of other metal ions on the glyphosate detection, Zn^{2+}, Fe^{3+}, Pb^{2+}, Ni^{2+}, Mg^{2+}, Mn^{2+}, Ca^{2+}, Al^{3+}, Hg^{2+}, and Co^{2+} at a ten times higher concentration (600 nM) than Cu^{2+}(60 nM) were tested under the same conditions. As shown in Figure 9, the fluorescence of the DNa2-Ag NCs was greatly quenched by the Cu^{2+} and Hg^{2+}. The results showed that the glyphosate could selectively bind to the Cu^{2+}, and most metal ions would not interfere with the detection of glyphosate, except Hg^{2+}. Since the pollution limit of Hg^{2+} in water is much lower than other metal ions, there is a low possibility of interference from Hg^{2+}.

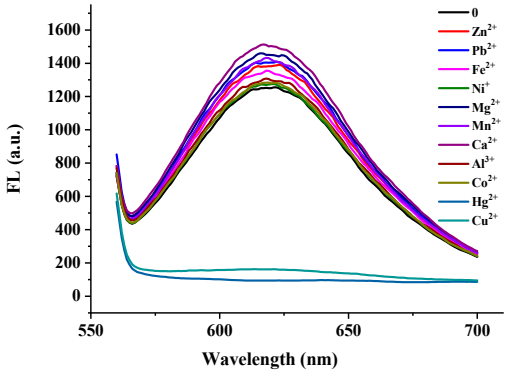

Figure 9. Fluorescence spectra of DNA2-Ag NCs in the presence of different metal ions.

The effects of the pH and Cu^{2+} concentration on the sensitivity of the sensing system were investigated. As shown in Figure 10A, when the pH value increased from 6 to 7.5, the fluorescence recovery $(F_2 - F_1)/F_2$ (F_1 and F_2 refer to the fluorescence of the DNA-Ag NCs/Cu^{2+} system in the absence and presence of glyphosate, respectively) gradually increased, and the highest fluorescence recovery rates were obtained at pH 7.5. The results indicated that the sensing system was more stable in weak alkaline environments. Therefore, Mops buffer (pH, 7.5) was selected for the subsequent experiments. The effect of the Cu^{2+} concentration was also investigated. As shown in Figure 10B, when the Cu^{2+} concentration was in the range of 40–100 nM, high fluorescence recovery of DNA-Ag NCs/Cu^{2+} could be obtained, and the highest recovery was obtained at 60 nM. Therefore, 60 nM Cu^{2+} was selected for glyphosate detection.

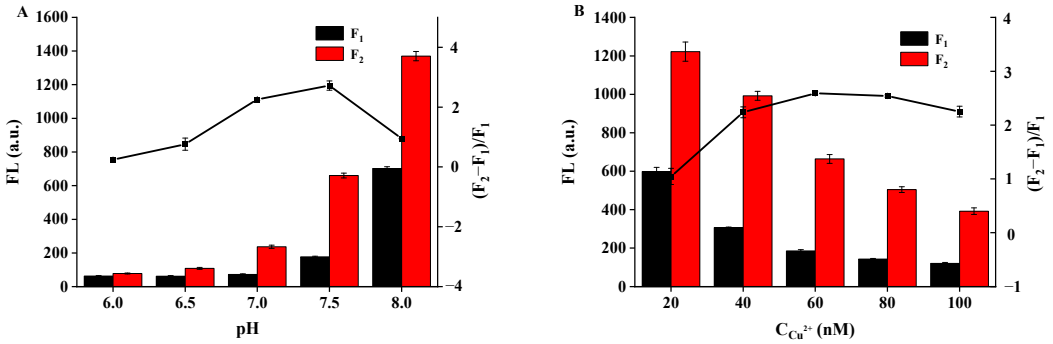

Figure 10. Effects of (**A**) pH and (**B**) different concentrations of Cu^{2+} on the recovery efficiency of DNA2-Ag NCs/Cu^{2+}/glyphosate.

4.5. Analytical Performance of the Glyphosate Detection

As shown in Figure 11, the fluorescence recovery, $(F_2 - F_1)/F_1$, gradually increased with the increased concentration of glyphosate in the range of 1.0 ng/mL~400 ng/mL, and a linear equation, $y = 0.058x + 0.081$ ($R^2 = 0.992$), was obtained in the range of 1–70 ng/mL. The LOD was calculated to be 0.2 ng/mL based on $3\sigma/s$ (σ is the standard deviation of the blank value and s is the slope of the equation).

Compared with some other typical fluorescence methods for the detection of glyphosate in recent years (Table 3), our proposed fluorescence detection method of glyphosate demonstrates much better sensitivity. Although Huang et al. constructed an ultrasensitive glyphosate fluorescence detection method using papain-coated gold nanoclusters as fluorescence probes combined with a tyrosinase/dopamine system [24], this method was relatively complex due to introducing a tyrosinase amplification system.

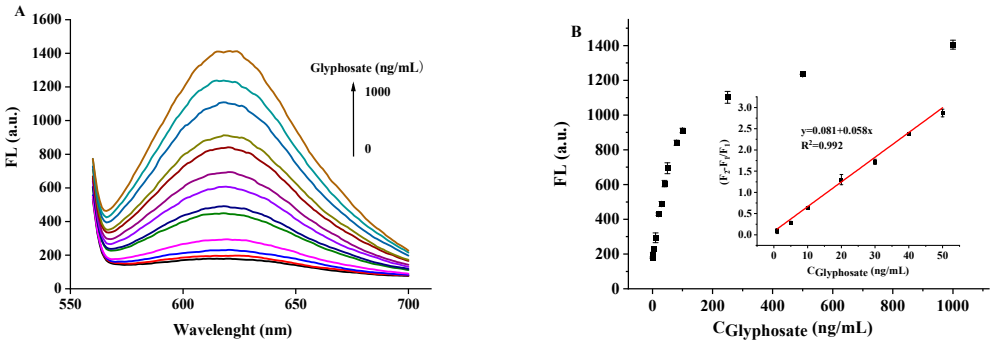

Figure 11. (**A**) The fluorescence recovery effect of DNA2-Ag NCs after adding different concentrations of glyphosate. (**B**) The relationship between the fluorescence intensity and different concentrations of glyphosate.

Table 3. Comparison of different methods used for detecting glyphosate.

Method	Linearity Range	LOD	Ref.
Electrochemistry	0.028~28 μg/mL	10 ng/mL	[25]
Chemiluminiscence	0.015~12 μg/mL	15 ng/mL	[26]
SERS	0.016~16 μg/mL	2.4 ng/mL	[27]
Fluorescence colorimetric	/	0.69 ng/mL	[28]
LFA	0.005~50 μg/mL	2 ng/mL	[29]
Fluorescence	0.1~1 μg/mL	7.8 ng/mL	[30]
Fluorescence	0.3~3 μg/mL	100 ng/mL	[31]
Fluorescence	0.04~0.4 ng/mL	0.035 ng/mL	[32]
Fluorescence	/	13 ng/mL	[33]
Fluorescence	1~50 ng/mL	0.2 ng/mL	This method

4.6. Selectivity Analysis

To evaluate the selectivity of the proposed method, eight more common pesticides including isocarbophos, phosalone, dimethoate, chlorpyrifos, fenamiphos, imidacloprid, acetamidine, and carbofuran at a five times higher concentration (1250 ng/mL) than glyphosate (250 ng/mL) were tested under the optimal conditions. As shown in Figure 12, the DNA2-Ag NCs/Cu^{2+} fluorescence sensing system did not respond to these high concentrations of pesticides, which indicated the excellent selectivity of that sensing system.

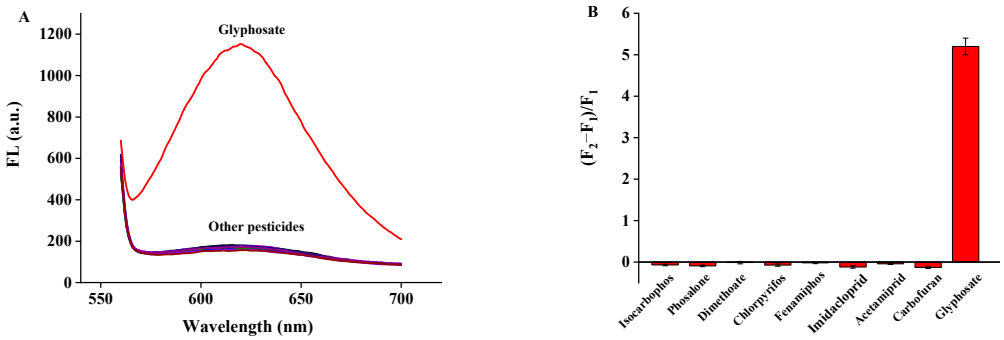

Figure 12. Selectivity of the assay for various pesticides. (**A**) Fluorescence; (**B**) pesticides.

4.7. Mechanism of Glyphosate Sensing

The quenching fluorescence of DNA-Ag NCs by Cu^{2+} was mainly ascribed to the interaction of Cu^{2+} with the phosphate base in the DNA [34]. To confirm this, EDTA, a strong Cu^{2+} chelator [35], was used to challenge the fluorescence quenching by Cu^{2+}. As shown in Figure 13, the addition of EDTA restored most of the fluorescence emissions, which indicated that complexation was the main reason. The surfaces of Cu^{2+} and DNA2-Ag NCs neutralized part of the negative charge of the DNA template, thereby quenching

the fluorescence of the DNA2-Ag NCs through electron or energy transfer processes [36]. At the same time, there may be another effect in the above fluorescence quenching, which we speculated was a metalphilic interaction between the copper and silver [37].

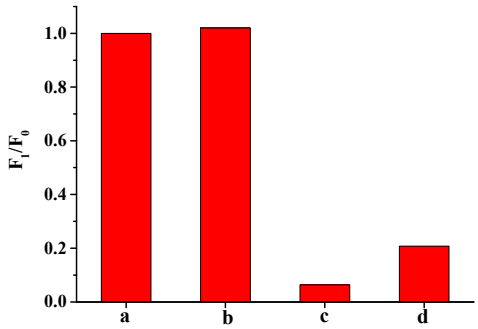

Figure 13. The fluorescence ratios of (a) DNA2-Ag NCs, (b) DNA2-Ag NCs/EDTA, (c) DNA2-Ag NCs/Cu^{2+}, and (d) DNA2-Ag NCs/Cu^{2+}/EDTA.

From the circular dichroism spectrum in Figure 14, the DNA2-Ag NCs have positive and negative absorption peaks at 275 nm and 245 nm, respectively, showing a typical B-type DNA conformation [14]. After the addition of Cu^{2+}, the absorption peaks at 245 nm and 275 nm obviously redshifted, which was associated with the changes in the DNA template microenvironment [38]. This result confirmed the occurrence of the interaction between the Cu^{2+} and oligonucleotide chains. Therefore, we hypothesized that both the carboxyl group (-COOH) and phosphonacyl group (-PO_3H_2) in the glyphosate chelated with Cu^{2+}, which destroyed the interaction between Cu^{2+} and DNA2-Ag NCs, resulting in the recovery of the DNA2-Ag NCs' fluorescence.

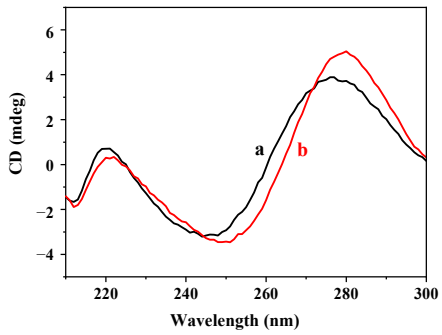

Figure 14. The circular dichroism spectra of (a) DNA2-Ag NCs and (b) DNA2-Ag NCs/Cu^{2+}.

5. Conclusions

In conclusion, a fluorescence turn-on sensor for glyphosate detection was constructed using DNA-Ag NCs. It was based on the Cu^{2+}-mediated strategy, in which Cu^{2+} can effectively quench the fluorescence of DNA-Ag NCs, and the coordination between the glyphosate and Cu^{2+} restored the fluorescence of the DNA-Ag NCs. The established method has the advantages of high sensitivity, simple operation, and low costs. The method was also used to detect glyphosate in tap water and spring water samples with satisfactory recovery. Our work provided a new option for the detection of glyphosate, and also showed that DNA-Ag NCs have high potential in pesticide detection.

Author Contributions: Y.C.: methodology, formal analysis, investigation, writing—original draft. G.L.: methodology, formal analysis, investigation, writing—original draft. X.H.: formal analysis, investigation, validation. Z.Q.: resources. C.P.: conceptualization, writing—review and editing, supervision, funding acquisition. All authors have read and agreed to the published version of the manuscript.

Funding: This work was supported by the National Natural Science Foundation of China (31871879) and Nanjing Customs Program (2021HK224).

Institutional Review Board Statement: Not applicable.

Informed Consent Statement: Not applicable.

Data Availability Statement: All data generated or analyzed during this study are included in this published article.

Conflicts of Interest: The authors have no competing interest to declare that are relevant to the content of this article and all authors declare they have no conflict of interest.

References

1. Ingaramo, P.; Alarcón, R.; Muñoz-De-Toro, M.; Luque, E.H. Are glyphosate and glyphosate-based herbicides endocrine disruptors that alter female fertility? *Mol. Cell. Endocrinol.* **2020**, *518*, 110934. [CrossRef] [PubMed]
2. Peillex, C.; Pelletier, M. The impact and toxicity of glyphosate and glyphosate-based herbicides on health and immunity. *J. Immunotoxicol.* **2020**, *17*, 163–174. [CrossRef] [PubMed]
3. Ighalo, J.O.; Ajala, O.J.; Adeniyi, A.G.; Babatunde, E.O.; Ajala, M.A. Ecotoxicology of glyphosate and recent advances in its mitigation by adsorption. *Environ. Sci. Pollut. Res.* **2021**, *28*, 2655–2668. [CrossRef]
4. Wang, S.; Liu, B.; Yuan, D.; Ma, J. A simple method for the determination of glyphosate and aminomethylphosphonic acid in seawater matrix with high performance liquid chromatography and fluorescence detection. *Talanta* **2016**, *161*, 700–706. [CrossRef] [PubMed]
5. Arkan, T.; Csámpai, A.; Molnár-Perl, I. Alkylsilyl derivatization of glyphosate and aminomethylphosphonic acid followed by gas chromatography mass spectrometry. *Microchem. J.* **2016**, *125*, 219–223. [CrossRef]
6. Chen, F.; Lu, Q.; Huang, L.; Liu, B.; Liu, M.; Zhang, Y.; Liu, J. DNA Triplex and Quadruplex Assembled Nanosensors for Correlating K^+ and pH in Lysosomes. *Angew. Chem. Int. Ed.* **2020**, *60*, 5453–5458. [CrossRef] [PubMed]
7. Yang, M.; Chen, X.; Su, Y.; Liu, H.; Zhang, H.; Li, X.; Xu, W. The Fluorescent Palette of DNA-Templated Silver Nanoclusters for Biological Applications. *Front. Chem.* **2020**, *8*, 601621. [CrossRef]
8. Wang, J.; Zhang, Z.; Gao, X.; Lin, X.; Liu, Y.; Wang, S. A single fluorophore ratiometric nanosensor based on dual-emission DNA-templated silver nanoclusters for ultrasensitive and selective Pb2+ detection. *Sens. Actuators B Chem.* **2019**, *282*, 712–718. [CrossRef]
9. Dadmehr, M.; Karimi, M.A.; Korouzhdehi, B. A signal-on fluorescence based biosensing platform for highly sensitive detection of DNA methyltransferase enzyme activity and inhibition. *Spectrochim. Acta Part A Mol. Biomol. Spectrosc.* **2020**, *228*, 117731. [CrossRef]
10. Li, M.; Xu, X.; Zhou, Z.; Xu, G.; Xie, Y.; Cai, Q. Label-free detection of microRNA: Two-stage signal enhancement with hairpin assisted cascade isothermal amplification and light-up DNA-silver nanoclusters. *Mikrochim. Acta* **2020**, *187*, 141. [CrossRef]
11. Yan, Z.; Tian, C.; Sun, X.; Wu, Y.; Li, D.; Ye, B. Ratiometric detection of biothiols by using the DNA-templated silver nanoclusters–Hg^{2+} system. *Anal. Methods* **2018**, *10*, 706–712. [CrossRef]
12. Yuan, Z.; Chen, Y.-C.; Li, H.-W.; Chang, H.-T. Fluorescent silver nanoclusters stabilized by DNA scaffolds. *Chem. Commun.* **2014**, *50*, 9800–9815. [CrossRef] [PubMed]
13. Zhang, M.; Ye, B.-C. Label-free fluorescent detection of copper(ii) using DNA-templated highly luminescent silver nanoclusters. *Anal.* **2011**, *136*, 5139–5142. [CrossRef] [PubMed]
14. Li, W.; Chen, X.; Fu, Y.; Zhang, J. Enantioselective Recognition Mechanism of Ofloxacin via Cu(II)-Modulated DNA. *J. Phys. Chem. B* **2014**, *118*, 5300–5309. [CrossRef] [PubMed]
15. Liu, J. DNA-stabilized, fluorescent, metal nanoclusters for biosensor development. *TrAC Trends Anal. Chem.* **2014**, *58*, 99–111. [CrossRef]
16. Ono, A.; Cao, S.; Togashi, H.; Tashiro, M.; Fujimoto, T.; Machinami, T.; Oda, S.; Miyake, Y.; Okamoto, I.; Tanaka, Y. Specific interactions between silver(i) ions and cytosine–cytosine pairs in DNA duplexes. *Chem. Commun.* **2008**, *39*, 4825–4827. [CrossRef] [PubMed]
17. Zhou, W.; Zhu, J.; Fan, D.; Teng, Y.; Zhu, X.; Dong, S. A Multicolor Chameleon DNA-templated Silver Nanocluster and Its Application for Ratiometric Fluorescence Target Detection with Exponential Signal Response. *Adv. Funct. Mater.* **2017**, *27*, 46. [CrossRef]
18. Richards, C.I.; Choi, S.; Hsiang, J.-C.; Antoku, Y.; Vosch, T.; Bongiorno, A.; Tzeng, Y.-L.; Dickson, R.M. Oligonucleotide-Stabilized Ag Nanocluster Fluorophores. *J. Am. Chem. Soc.* **2008**, *130*, 5038–5039. [CrossRef]
19. Shah, P.; Choi, S.W.; Nagda, R.; Geczy, R.; Cho, S.K.; Bhang, Y.J.; Kim, T.-H.; Song, T.Y.; Lee, P.H.; Kang, J.-H.; et al. The structural shift of a DNA template between a hairpin and a dimer tunes the emission color of DNA-templated AgNCs. *Nanoscale* **2018**, *10*, 20717–20722. [CrossRef]
20. Deiana, M.; Matczyszyn, K.; Massin, J.; Olesiak-Banska, J.; Andraud, C.; Samoc, M. Interactions of Isophorone Derivatives with DNA: Spectroscopic Studies. *PLoS ONE* **2015**, *10*, e0129817. [CrossRef]

21. Ware, W.R. Oxygen quenching of fluorescence in solution: An experimental study of the diffusion process. *J. Phys. Chem.* **1962**, *66*, 455–458. [CrossRef]
22. Shakir, M.; Azam, M.; Parveen, S.; Khan, A.U.; Firdaus, F. Synthesis and spectroscopic studies on complexes of N,N′-bis-(2-pyridinecarboxaldimine)-1,8-diaminonaphthalene (L); DNA binding studies on Cu(II) complex. *Spectrochim. Acta Part A Mol. Biomol. Spectrosc.* **2009**, *71*, 1851–1856. [CrossRef] [PubMed]
23. Madsen, H.E.L.; Christensen, H.H.; Gottlieb-Petersen, C.; Andresen, A.F.; Smidsrød, O.; Pontchour, C.-O.; Phavanantha, P.; Pramatus, S.; Cyvin, B.N.; Cyvin, S.J. Stability Constants of Copper(II), Zinc, Manganese(II), Calcium, and Magnesium Complexes of N-(Phosphonomethyl)glycine (Glyphosate). *Acta Chem. Scand.* **1978**, *32*, 79–83. [CrossRef]
24. Liu, Q.; Zhou, Q.; Jiang, G. Nanomaterials for analysis and monitoring of emerging chemical pollutants. *TrAC Trends Anal. Chem.* **2014**, *58*, 10–22. [CrossRef]
25. Chiu, H.-Y.; Lin, Z.-Y.; Tu, H.-L.; Whang, C.-W. Analysis of glyphosate and aminomethylphosphonic acid by capillary electrophoresis with electrochemiluminescence detection. *J. Chromatogr. A* **2008**, *1177*, 195–198. [CrossRef] [PubMed]
26. Qin, Y.; Wu, G.; Guo, Y.; Ke, D.; Yin, J.; Wang, D.; Fan, X.; Liu, Z.; Ruan, L.; Hu, Y. Engineered glyphosate oxidase coupled to spore-based chemiluminescence system for glyphosate detection. *Anal. Chim. Acta* **2020**, *1133*, 39–47. [CrossRef]
27. Xu, M.-L.; Gao, Y.; Li, Y.; Li, X.; Zhang, H.; Han, X.X.; Zhao, B.; Su, L. Indirect glyphosate detection based on ninhydrin reaction and surface-enhanced Raman scattering spectroscopy. *Spectrochim. Acta Part A Mol. Biomol. Spectrosc.* **2018**, *197*, 78–82. [CrossRef]
28. Guan, J.; Yang, J.; Zhang, Y.; Zhang, X.; Deng, H.; Xu, J.; Wang, J.; Yuan, M.-S. Employing a fluorescent and colorimetric picolyl-functionalized rhodamine for the detection of glyphosate pesticide. *Talanta* **2021**, *224*, 121834. [CrossRef]
29. Sawetwong, P.; Chairam, S.; Jarujamrus, P.; Amatatongchai, M. Enhanced selectivity and sensitivity for colorimetric determination of glyphosate using Mn–ZnS quantum dot embedded molecularly imprinted polymers combined with a 3D-microfluidic paper-based analytical device. *Talanta* **2021**, *225*, 122077. [CrossRef]
30. Wang, X.; Yang, Y.; Huo, D.; Ji, Z.; Ma, Y.; Yang, M.; Luo, H.; Luo, X.; Hou, C.; Lv, J. A turn-on fluorescent nanoprobe based on N-doped silicon quantum dots for rapid determination of glyphosate. *Mikrochim. Acta* **2020**, *187*, 341. [CrossRef]
31. Yuan, Y.; Jiang, J.; Liu, S.; Yang, J.; Zhang, H.; Yan, J.; Hu, X. Fluorescent carbon dots for glyphosate determination based on fluorescence resonance energy transfer and logic gate operation. *Sensors Actuators B Chem.* **2017**, *242*, 545–553. [CrossRef]
32. Hong, C.; Ye, S.; Dai, C.; Wu, C.; Chen, L.; Huang, Z. Sensitive and on-site detection of glyphosate based on papain-stabilized fluorescent gold nanoclusters. *Anal. Bioanal. Chem.* **2020**, *412*, 8177–8184. [CrossRef] [PubMed]
33. Gui, M.; Jiang, J.; Wang, X.; Yan, Y.; Li, S.; Xiao, X.; Liu, T.; Liu, T.; Feng, Y. Copper ion-mediated glyphosate detection with N-heterocycle based polyacetylene as a sensing platform. *Sensors Actuators B Chem.* **2017**, *243*, 696–703. [CrossRef]
34. Wang, R.; Yan, X.; Sun, J.; Wang, X.; Zhao, X.-E.; Liu, W.; Zhu, S. Cu^{2+} modulated DNA-templated silver nanoclusters as a turn-on fluorescence probe for the detection of quinolones. *Anal. Methods* **2018**, *10*, 4183–4188. [CrossRef]
35. Huang, X.-F.; Ren, B.-X.; Peng, C.-F.; Wei, X.-L.; Xie, Z.-J. Fluorescent sensing of mercury (II) and copper (II) ions based on DNA-templated Cu/Ag nanoclusters. *Microchem. J.* **2020**, *158*, 105214. [CrossRef]
36. Zheng, X.; Yao, T.; Zhu, Y.; Shi, S. Cu^{2+} modulated silver nanoclusters as an on–off–on fluorescence probe for the selective detection of l-histidine. *Biosens. Bioelectron.* **2015**, *66*, 103–108. [CrossRef]
37. Li, S.; Cao, W.; Kumar, A.; Jin, S.; Zhao, Y.; Zhang, C.; Zou, G.; Wang, P.C.; Li, F.; Liang, X.-J. Highly sensitive simultaneous detection of mercury and copper ions by ultrasmall fluorescent DNA–Ag nanoclusters. *New J. Chem.* **2014**, *38*, 1546–1550. [CrossRef]
38. Zhang, P.; Wang, Y.; Chang, Y.; Xiong, Z.H.; Huang, C.Z. Highly selective detection of bacterial alarmone ppGpp with an off–on fluorescent probe of copper-mediated silver nanoclusters. *Biosens. Bioelectron.* **2013**, *49*, 433–437. [CrossRef]